Progress In Electromagnetics Research M, Vol. 32, 229–244, 2013

SURFACE ELECTROMAGNETIC WAVES IN FINITE SEMICONDUCTOR-DIELECTRIC PERIODIC STRUCTURE IN AN EXTERNAL MAGNETIC FIELD

Vladislava V. Baibak[1], Illia V. Fedorin[2, *], and Aleksey A. Bulgakov[1]

[1]Institute for Radiophysics and Electronics, National Academy of Science of Ukraine, 12, Ak. Proskura Str., Kharkiv UA-61085, Ukraine

[2]National Technical University "Kharkiv Polytechnical Institute", 21, Frunze Str., Kharkiv UA-61002, Ukraine

Abstract—The specific features of TM-polarized surface electromagnetic waves in a finite structure fabricated by a periodic alternating semiconductor and dielectric layers are investigated. Dispersion characteristics of eigenwaves are analyzed numerically and analytically. The complex Poynting energy flux and the surface wave's distribution are calculated. The influence of geometrical and physical parameters of the structure on the properties of surface waves is studied.

1. INTRODUCTION

The terahertz (THz) regime is that promising slice of the electromagnetic (EM) spectrum that lies between the microwave and the optical, corresponding to frequencies of about $10^{12} \ldots 10^{13}$ hertz. Feature of THz spectrum range is that its inherent wavelength is too long to be used in a well-developed optical technology and yet is too short for transferring radio methods into it. Classical electrodynamics and electronics are used for analytical describing of physical processes in the microwave, infrared and at shorter frequency ranges — the methods that correspond to quantum electronics and optics. Submillimeter waves are at the junction between these studies [1].

THz radiation does have some uniquely attractive qualities. For example, it can yield extremely high-resolution images and move vast amounts of data quickly. The waves also stimulate molecular

Received 23 July 2013, Accepted 19 August 2013, Scheduled 24 August 2013
* Corresponding author: Illia V. Fedorin (fedorin.ilya@gmail.com).

and electronic motions in many materials — reflecting off some, propagating through others, and being absorbed by the rest [1]. Nowadays many researchers struggle with challenge of turning such phenomena into real-world applications [2–6]. Compared to the relatively well-developed science and technology at microwave, optical and x-ray frequencies, basic research, new initiatives and advanced technology developments in the THz band are very limited and remain relatively unexplored [7].

At the same time, we believe that many technical problems can be solved through the use of periodic structures and metamaterials [8–10]. In recent years, there has been an increasing interest in development and fabrication of new type of materials with characteristics that may not be found in nature. Moreover, there has been also a remarkable attention to properties of materials which have either negative permittivity or permeability in some frequency range owing to their novel applications potential in microwave circuits [8, 11–15]. Examples are various types of artificial periodic structures of different nature, metamaterials, in particular negative index materials (NIM), chiral media, and composite materials. A broad range of applications has been suggested including artificial dielectrics, lenses, absorbers, antenna structures, optical and microwave components, sensors, and frequency selective surfaces [8, 10, 16, 17].

For effective practical application of such types of structures first of all we need to know how the EM waves behave in materials, how to construct and design such materials, what characteristics may be useful for practical applications and what new applications can be identified to utilize new wave characteristics [18]. This paper deals with the first of the above questions through the study of THz surface waves properties in the semiconductor periodic structure.

Surface EM waves (SW) are waves that propagate along the interface between differing media and decrease in the transverse direction exponentially. Having, in linear case, the field maximum on the interface, SW are a very sensitive and convenient tool for studying the surfaces physical properties. Thus, the studies of SW are of great importance for both fundamental and practical interest [19–22]. For example, it was shown recently that SW were responsible for the extraordinary high transmission through a silver film with subwavelength hole arrays and for the subdiffraction-limit focusing effect using a slab of negative index material. In some other situations, the absence of a SW is desired since its excitation costs unfavorable loss of energy and unwanted interference [23, 24].

In this regard, during the last few years, different fundamental issues have been addressed. Many significant papers have been devoted to SW at the interfaces between periodic structures and metamaterials [25–36]. While tremendous progress has been made in the physics and practical applications of periodic structures and metamaterials, the effects associated with the influence of external fields in complex composites still remain relatively unexplored.

For further clarification of interesting properties of multilayer periodic structures and metamaterials, we present in this paper a comprehensive analysis of SW existence at the interface between a finite semiconductor-dielectric periodic structure in an external magnetic field and two semi-infinite isotropic media. We concentrate our attention here on the properties of SW in the terahertz range.

The purpose of this paper is to identify the ranges of TM-polarized SW existence depending on system parameters and to study in more details their peculiar features in the considered structure. In our paper we have shown that the properties of SW in such structure depend heavily on the permittivity tensor components of the constitutive layers, thicknesses of the layers, operating frequency, and external magnetic field. Moreover, we have shown that SW at different interfaces have quite rich different spectra with different properties, the study of which provide additional information about unique properties of such types of materials. To get deeper insight into the physics of such waves, we have calculated their complex Poynting energy flux along with the dispersion law.

2. GEOMETRY OF THE STRUCTURE. BASIC EQUATIONS

Let us consider a layered periodic structure that consists of alternate semiconductor and dielectric layers of thickness d_1 and d_2, and permittivities ε^s and ε_2, respectively. We assume that the thickness of the structure is L ($L = Nd$, where N is the number of periods, $d = d_1 + d_2$ is the period of the structure). We introduce a coordinate system such that the x-axis is parallel to the boundaries of the layers and z-axis is perpendicular to the layers. The structure is placed into an external magnetic field H_0 along y-axis (Fig. 1). We suppose that the structure is homogeneous in the x and y directions and we put $\partial/\partial y = 0$. Then, Maxwell's equations split into two independent modes or polarizations. The first mode is the transverse magnetic (TM) with E_x, H_y, E_z EM field components and the second is the transverse electric (TE) with H_x, E_y, H_z EM field components. Since the expressions for the TE-polarization are independent of the external magnetic field, and, moreover, for TE waves SW do not exist, we further consider only the TM-polarization.

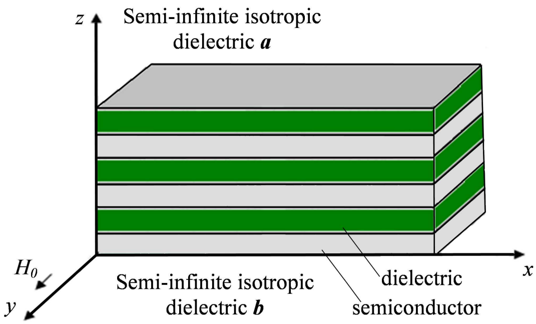

Figure 1. Geometry of the periodic structure.

To solve the problem, we use Maxwell's equations in the semiconductor and dielectric layers, the equations of continuity and the motion of charge carriers. We seek the variables in these equations in the form of $\exp[ik_x x + ik_z z - i\omega t]$. We also apply boundary conditions for the tangential field components at the layer interfaces.

The permittivity of semiconductor layer is a tensor for the investigated THz region. It can be given as [9]

$$\varepsilon^s = \begin{pmatrix} \varepsilon^s_{xx} & 0 & \varepsilon^s_{xz} \\ 0 & \varepsilon^s_{yy} & 0 \\ \varepsilon^s_{zx} & 0 & \varepsilon^s_{zz} \end{pmatrix}, \tag{1}$$

where

$$\begin{aligned} (\varepsilon^s_{xx}) &= (\varepsilon^s_{zz}) = \varepsilon_{\parallel} = \varepsilon_{01}\left(1 - \frac{\omega_P^2(\omega + i\nu)}{\omega\left[(\omega + i\nu)^2 - \omega_C^2\right]}\right), \\ (\varepsilon^s_{xz}) &= -(\varepsilon^s_{zx}) = \varepsilon_{\perp} = -i\varepsilon_{01}\left(\frac{\omega_P^2\omega_C}{\omega\left[(\omega + i\nu)^2 - \omega_C^2\right]}\right), \\ (\varepsilon^s_{yy}) &= \varepsilon_{01}\left(1 - \frac{\omega_P^2}{\omega(\omega + i\nu)}\right). \end{aligned} \tag{2}$$

Here ε_{01} is the permittivity part attributed to the lattice, ω_P is the plasma frequency, ω_C is the cyclotron frequency and ν is the collision frequency. The permeability for nonmagnetic semiconductor and dielectric layers is $\mu = 1$.

The dispersion relation for TM waves in the infinite periodic structure, which relates the frequency ω, the longitudinal wave number

k_x and the Bloch wave number $\bar{k}$, can be written as [9]

$$\cos\bar{k}d = \cos k_{z1}d_1 \cos k_{z2}d_2 - \frac{\varepsilon_{f1}\varepsilon_2}{2k_{z1}k_{z2}} \times \left(\left(\frac{k_{z1}}{\varepsilon_{f1}}\right)^2 + \left(\frac{k_{z2}}{\varepsilon_2}\right)^2 - \left(\frac{k_x}{\varepsilon_{f1}}\frac{\varepsilon_\perp}{\varepsilon_\parallel}\right)^2 \right) \sin k_{z1}d_1 \sin k_{z2}d_2, \quad (3)$$

where $k_{z1,2} = ((\omega/c)^2\varepsilon_{f1,2} - k_x^2)^{1/2}$ are the transversal wave numbers of the semiconductor and dielectric layers, respectively; the Bloch wave number $\bar{k}$ is an effective transverse wave number that characterizes the periodicity of the structure; $\varepsilon_{f1} = \varepsilon_\parallel + \varepsilon_\perp^2/\varepsilon_\parallel$ is the Voigt effective permittivity of the semiconductor layer.

3. ANALYTICAL AND NUMERICAL INVESTIGATION OF DISPERSION RELATION FOR AN INFINITE PERIODIC STRUCTURE

The dispersion relation (3) defines the band structure of the infinite periodic media. Let us assume that the collision frequency in the semiconductor is zero ($\nu = 0$) and the losses in the dielectric can be neglected. The numerical simulation was carried out for the layered structure consisting 4 periods ($N = 4$) of alternating layers with the following parameters: the first layer is an *n-InSb* type semiconductor ($\varepsilon_{01} = 17.8$, $d_1 = 70\,\mu\text{m}$, $\omega_P = 1.6 \times 10^{12}\,\text{s}^{-1}$) and the second layer is a SiO_2 dielectric ($\varepsilon_2 = 4.0$, $d_2 = 30\,\mu\text{m}$). These materials have a great applied interest for microwave applications. Among III–V family of binary semiconductors indium antimonide has the smallest band gap and the smallest effective mass of conduction electrons. Moreover, since InSb has a record value of room-temperature electron mobility, InSb-based devices are attractive for field effect transistors, magnetic field sensors, ballistic transport devices, and other applications where the performance depends on a high mobility or a long mean free path. On the other hand, quartz (SiO_2) crystals are widely used in today's electronics as high quality tuned circuits or resonators [9].

The analytical analysis of dispersion Equation (3) reveals 3 characteristic frequencies:

$$\omega_{01,02} = \mp\frac{\omega_C}{2} + \left(\frac{\omega_C^2}{4} + \omega_{ps}^2\right)^{1/2} \quad \text{and} \quad \omega_g = \left(\omega_P^2 + \omega_C^2\right)^{1/2}, \quad (4)$$

where $\omega_{ps} = \omega_P\sqrt{\varepsilon_{01}/(\varepsilon_{01} + \varepsilon_2)}$ is the surface plasmon frequency at the semiconductor-dielectric interfaces; at the hybrid resonance frequency ω_g the (ε_{xx}^p) component of the semiconductor permittivity tensor diverges and $\varepsilon_{f1} \to \pm\infty$.

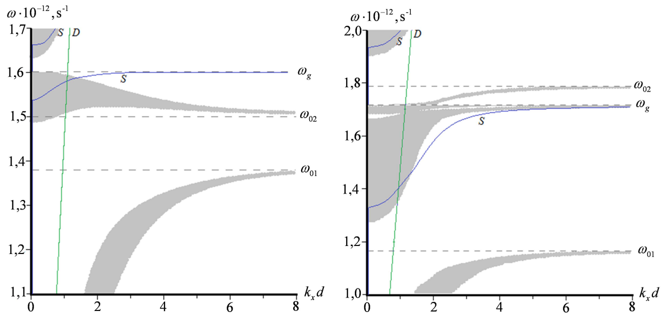

(a) (b)

Figure 2. Band structure of the infinite layered periodic media in the case of weak ((a) $H_0 = 7.9\,\text{kA/m}$) and strong magnetic fields ((b) $H_0 = 39.8\,\text{kA/m}$).

The band structure of the spectrum for different values of magnetic field H_0 is depicted in Fig. 2 (the transmission bands are indicated by hatching). In the case of weak magnetic fields, when $\omega_C < \omega_{cr} = \omega_{ps}(\varepsilon_2/\varepsilon_{01})\sqrt{\varepsilon_{01}/(\varepsilon_{01}-\varepsilon_2)}$, characteristic frequencies for the "acoustic" (ω_{01}) and "optical" (ω_{02}) branches of surface magnetoplasmons are below the hybrid frequency, that is $\omega_{01} < \omega_{02} < \omega_g$ (see Fig. 2(a)). On the contrary, in the case of strong magnetic fields, when $\omega_C > \omega_{cr}$: $\omega_{01} < \omega_g < \omega_{02}$ (see Fig. 2(b)).

SW existence at the interfaces between the layers of the periodic structure is connected with the position of light lines of semiconductor (i.e., $(\omega/c)\sqrt{\varepsilon_{f1}} = k_x$) and dielectric (i.e., $(\omega/c)\sqrt{\varepsilon_2} = k_x$). In Fig. 2 the dielectric light line is marked as line D, whereas the semiconductor light line is marked as S. When the allowed and forbidden bands are located to the right of the dielectric light line, the wave number k_{z2} is pure imaginary. Similarly for semiconductor. Thus, when the transverse wave numbers of the layers k_{z1}, k_{z2} are simultaneously imaginary, the EM waves have the surface nature in both layers. On the other hand, when the transverse wave number in one of the layers is purely real, whereas in another layer is purely imaginary, then the corresponding layers support bulk and exponentially damped waves, respectively. And, finally, when both wave numbers are purely real, each layer of the periodic structure supports only bulk waves.

A complete analysis of the infinite periodic media band structure can be found in [37].

4. DISPERSION RELATION FOR SW IN THE LAYERED PERIODIC STRUCTURE OF FINITE LENGTH

Surface nature of EM field distribution in the layers of the structure is associated with the negative value of permittivity in one of the layers, and, consequently, with the imaginary values of wave numbers [20]. However, the possibility of SW existence on the interfaces between the entire multilayer periodic structure and surrounding half-spaces can be considered only when the Bloch wave number is imaginary.

Now consider the case when the finite multilayered periodic structure is placed between two homogeneous media with the permittivities ε_a and ε_b. Transverse wave numbers in media a and b should be purely imaginary and take the form:

$$k_{za} = -i\left(k_x^2 - \frac{\omega^2}{c^2}\varepsilon_a\right)^{1/2}, \quad k_{zb} = i\left(k_x^2 - \frac{\omega^2}{c^2}\varepsilon_b\right)^{1/2}. \tag{5}$$

Such a choice of signs in (5) ensures that the wave amplitudes decrease exponentially on both interfaces between the multilayer periodic structure and two semi-infinite dielectric media.

To describe the finite in the z-direction periodic structure we use the Abeles' theory and raise the transfer matrix $\mathbf{m}$ for one period (expressions for the components of this matrix are textbook values and they can be found, for example, in [9]) to the N-th power

$$\begin{pmatrix} H_y(0) \\ E_x(0) \end{pmatrix} = \mathbf{M}_N \begin{pmatrix} H_y(Nd) \\ E_x(Nd) \end{pmatrix}, \quad \mathbf{M}_N = (\mathbf{m})^N. \tag{6}$$

Using the Abeles' theorem, the matrix $\mathbf{M}_N$ for N periods of the structure can be written as Chebyshev polynomials of second kind [9].

We represent the wave functions within the periodic structure in the form of Bloch functions. Taking into account the boundary conditions for tangential components of the EM field at $z = 0$ and $z = Nd$, we arrive at the system of homogeneous linear equations:

$$\begin{pmatrix} A \\ -\frac{c}{\omega}\frac{k_{za}}{\varepsilon_a}A \end{pmatrix} = \mathbf{M}_N \begin{pmatrix} De^{ik_{zb}Nd} \\ \frac{c}{\omega}\frac{k_{zb}}{\varepsilon_b}De^{ik_{zb}Nd} \end{pmatrix}. \tag{7}$$

Here A and D are indefinite coefficients. A non-trivial solution of (7) exists only if the determinant of the system is zero, and, in this way, we obtain the following dispersion relation for SW in the finite periodic structure:

$$\left[m_{11} + \frac{|k_{zb}|}{|k_{za}|}\frac{\varepsilon_a}{\varepsilon_b}m_{22} + i\left(\frac{c}{\omega}\frac{|k_{zb}|}{\varepsilon_b}m_{12} - \frac{\omega}{c}\frac{\varepsilon_a}{|k_{za}|}m_{21}\right)\right] \times\frac{\sin\left(N\bar{k}d\right)}{\sin\left(\bar{k}d\right)} - \left[1 + \frac{|k_{zb}|}{|k_{za}|}\frac{\varepsilon_a}{\varepsilon_b}\right]\frac{\sin\left(\left[N-1\right]\bar{k}d\right)}{\sin\left(\bar{k}d\right)} = 0. \tag{8}$$

This equation relates the propagation constant of SW k_x and frequency ω. Assume that the periodic structure is placed into the vacuum, so that $\varepsilon_a = \varepsilon_b = \varepsilon_v = 1$, and $k_{za} = k_{zb} = k_{z\text{v}}$. In this case the dispersion relation (8) can be significantly simplified:

$$\frac{\sin\left(N\bar{k}d\right)}{\sin\left(\bar{k}d\right)} + \frac{\sin\left(\left[N-1\right]\bar{k}d\right)}{2\sin\left(\bar{k}d\right)}\left[\frac{c}{\omega}\frac{|k_{z\text{v}}|}{\varepsilon_\text{v}}im_{12} + \frac{\omega}{c}\frac{\varepsilon_\text{v}}{|k_{z\text{v}}|}im_{21}\right] = 0. \quad (9)$$

From (9) it also follows a well-known physical result, that the dispersion relation has N roots for each transmission band of periodic structure [38].

In the electrostatic case, when $k_x \gg \omega/c$, using the equations for the transverse wave numbers of the layers, the dispersion relation (9) for SW can be reduced to

$$\left(\varepsilon_\parallel - i\varepsilon_\perp + \varepsilon_2\right)\left(\varepsilon_\parallel + i\varepsilon_\perp + \varepsilon_\text{v}\right) = 0. \quad (10)$$

The Equation (10) is independent of the spatial dispersion, period of the structure, thicknesses of the layers and number of periods N. As the result, we have two surface modes. As before, let us define them as an acoustic and an optical surface mode. It is evident that the acoustic mode depends on the permittivity of semiconductor and dielectric, whereas the optical mode is associated with the permittivity of semiconductor and vacuum.

From the dispersion Equation (10) we obtain two characteristic frequencies for the acoustic and optical surface modes in the electrostatic approximation:

$$\omega_{s1} = \omega_{01} = -\frac{\omega_C}{2} + \sqrt{\frac{\omega_C^2}{4} + \frac{\omega_P^2\varepsilon_{01}}{\varepsilon_{01}+\varepsilon_2}}, \quad \omega_{s2} = \frac{\omega_C}{2} + \sqrt{\frac{\omega_C^2}{4} + \frac{\omega_P^2\varepsilon_{01}}{\varepsilon_{01}+\varepsilon_v}}. \quad (11)$$

Thus, in the electrostatic case, the ranges of surface modes existence depend only on the magnetic field, frequency, parameters of materials forming the periodic structure and permittivities of surrounding media.

Figure 3 shows the results of numerical calculations of the dispersion relation (9). It should be noted that all dispersion curves of SW lie to the right of the vacuum light line (i.e., $(\omega/c)\sqrt{\varepsilon_\text{v}} = k_x$, line V) and in the forbidden bands of periodic structure, due to the imaginary values of the vacuum transversal wave number k_{zv}, and Bloch wave number $\bar{k}$.

In Fig. 3 the black solid lines are the surface modes. As is generally known, in the finite periodic structure instead of transmission bands, we are dealing with the waveguide modes. In the considered THz frequency range there are $(N-1)$ modes within the transmission band and one is a SW mode [38].

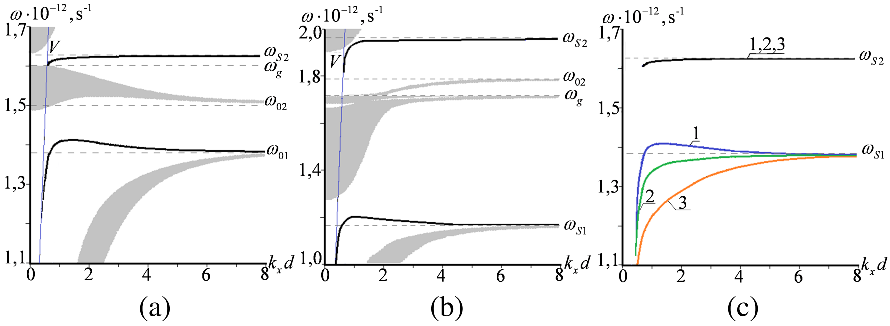

Figure 3. Dispersion curves for surface modes in the case of weak ((a) $H_0 = 7.9\,\text{kA/m}$) and strong magnetic fields ((b) $H_0 = 39.8\,\text{kA/m}$); for various thicknesses of the layers ((c) $d = 0.01\,\text{cm}$): 1 — $d_1/d_2 = 7/3$, 2 — $d_1/d_2 = 1$, 3 — $d_1/d_2 = 3/7$.

As can be seen, the external magnetic field does not affects the shape of the surface modes curves, whereas only affects the values of characteristic frequencies $\omega_{01,02}$ and $\omega_{s1,s2}$. It should be noted that the acoustic surface mode tends asymptotically to the frequency ω_{s1}, whereas below this frequency it changes monotonously along the vacuum light line. At the same time, the optical surface mode tends asymptotically to the characteristic frequency ω_{s2}. Fig. 3(c) shows the dispersion relation of surface modes versus the ratio of the layer thicknesses d_1/d_2. It is obviously that when the dielectric layer thickness d_2 is greater than the semiconductor layer thickness d_1 the dispersion curve lies closer to the transmission band (curve 3). In the opposite case, the dispersion curve becomes steeper (curve 1). For the optical surface mode the dependency of d_1/d_2 is negligible. Note also, that for $k_x \to \infty$, the width of the transmission bands tends to zero and, according to (10), the ratio of the layer thicknesses has no impact, and both surface modes tend asymptotically to the corresponding characteristic frequencies ω_{s1} and ω_{s2}.

Thus, SW can be supported by a finite multilayer periodic structure in specific frequency ranges. Effective control of SW parameters is possible by means of altering the parameters of the layers forming the periodic structure. Moreover, as shown above, the transverse wave numbers of the layers of the unit cells can be both real and imaginary, so that within the layers both bulk and exponentially decaying waves may propagate. However, the resultant Bloch wave has the surface nature.

5. EM FIELD DISTRIBUTION AND ENERGY FLUX OF SW

Here, we show that in the considered periodic structure there are two independent SW, localized near the interfaces between the vacuum and periodic structure.

To this end, let us consider the EM field distribution in the periodic structure and the imaginary part of the Poynting vector. It is generally known, that the Poynting energy flux vector $\mathbf{S}$ is a complex quantity [39, 40]

$$\operatorname{div}\mathbf{S} = -\frac{1}{2}\sigma EE^* + i\omega\left(\frac{\mu}{2}HH^* - \frac{\varepsilon}{2}EE^*\right). \tag{12}$$

As stated in [39], the imaginary part of the complex Poynting theorem conveys additional information about physical processes within the periodic structure, as it is the difference between the time-averaged magnetic and electric energies.

Let us analyze the EM field distribution for acoustic surface mode for different values of ω and k_x. The calculations were performed for 4 periods ($N = 4$). The electric and magnetic field distribution in the whole multilayer periodic structure is a property of the EM waves interference. Nature of EM field interference in the periodic structure can be determined by means of the transfer matrix $\mathbf{M}_N$. No less helpful is to study the energy storage in the electric and magnetic fields [39].

Figure 4 shows the results of numerical calculations of the EM field distribution and the difference in the magnetic and electric field energies for three different values of ω and k_x.

As is evident from Fig. 4, depending on frequency ω and propagation constant of SW k_x, the EM field of SW may exist either at one of the boundaries of the periodic structure or at both boundaries simultaneously. These two SW are independent. The reasonable question is under what conditions and at what boundary SW occur?

To solve this problem it is convenient to consider the complex Poynting energy flux. Despite the fact that this quantity has no direct physical meaning, it allows us to say whether the waves are independent on both boundaries.

From Fig. 4, we can also see that when the electric and magnetic field energies are concentrated at the left boundary of the structure, the complex Poynting energy flux is concentrated at the same boundary (Fig. 4(a)). The similar behavior occurs at the right boundary of the structure (Fig. 4(c)) and, in the case, when there are two independent SW at both boundaries of the structure (Fig. 4(b)).

It should be noted that such antisymmetric behaviour of SW field and energy becomes possible due to the peculiarities of the

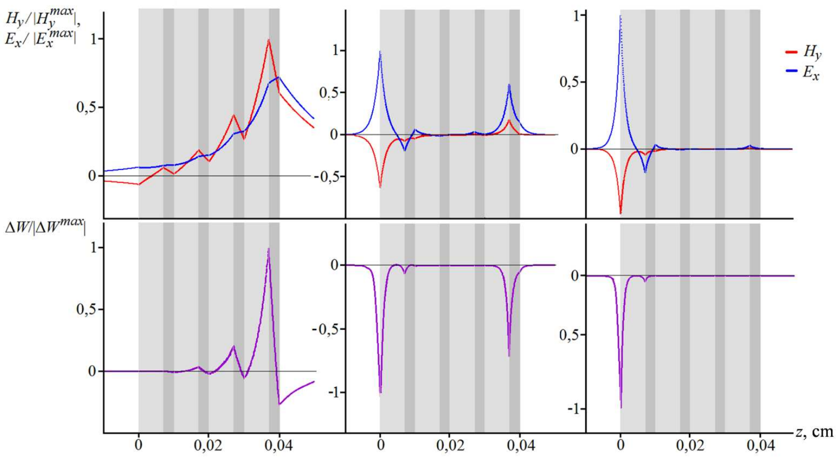

(a) (b) (c)

Figure 4. Normalized EM field (H_y and E_x) and complex energy flux ($\Delta W = (\frac{\mu}{2}HH^* - \frac{\varepsilon}{2}EE^*)$) distribution of SW ($H_0 = 7.9\,\text{kA/m}$). (a) $\omega = 1.41 \cdot 10^{12}\,\text{s}^{-1}$, $k_x = 110\,\text{cm}^{-1}$; (b) $\omega = 1.384 \cdot 10^{12}\,\text{s}^{-1}$, $k_x = 600\,\text{cm}^{-1}$; (c) $\omega = 1.382 \cdot 10^{12}\,\text{s}^{-1}$, $k_x = 785\,\text{cm}^{-1}$.

multilayer periodic structure, as well as the fact that the first (vacuum/semiconductor) and second (dielectric/vacuum) interfaces are various. If both interfaces are the same, then the distribution of SW field and energy flux will be symmetric.

6. PENETRATION DEPTH OF SW AND THE INFLUENCE OF DISSIPATION PROCESSES

Let us now consider the penetration depth (PD) δ of acoustic and optical SW modes versus frequency for various magnetic fields (Fig. 5, $d_1 = 70\,\mu\text{m}$, $d_2 = 30\,\mu\text{m}$, $N = 4$). The PD is the depth at which the intensity of the SW field inside the structure falls to $1/e$ (about 37%) of its original value at the surface. The PD into the periodic structure varies slightly and is within 20–140 microns for the acoustic surface mode and 10–90 microns for optical mode. So that, the maximum values of PD occur at a distance of one and a half periods of the structure, when the SW dispersion curves cross the dielectric light line.

Here, we examine how the dissipative processes affect the properties of SW. When the collisions in the semiconductor layer are taken into account, then the semiconductor permittivity tensor components (2), Bloch wave number, and SW propagation constant

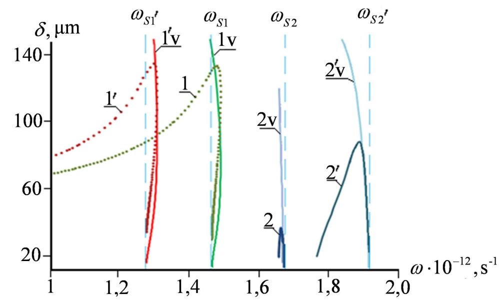

Figure 5. PD of acoustic (1, 1′) and optical (2, 2′) SW modes in the multilayer periodic structure and vacuum (index v) versus frequency at $H_0 = 7.9\,\text{kA/m}$ (1, 2) and $H_0 = 39.8\,\text{kA/m}$ (1′, 2′).

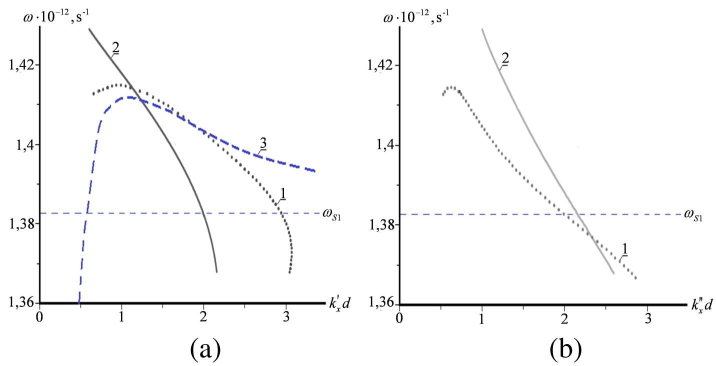

Figure 6. Dispersion curves for (a) real and (b) imaginary parts of SW propagation constant k_x for acoustic surface mode at $H_0 = 7.9\,\text{kA/m}$. 1 — $\nu = 5 \cdot 10^{10}\,\text{s}^{-1}$, 2 — $\nu = 1 \cdot 10^{11}\,\text{s}^{-1}$, 3 — $\nu = 0$.

are complex values: $\varepsilon = \varepsilon' + i\varepsilon''$, $k_x = k_x' + ik_x''$, $\bar{k} = \bar{k}' + i\bar{k}''$ [41].

Figure 6 shows the numerical calculations of SW dispersion curves for different values of collision frequency ν. The presence of losses in the structure leads to the dispersion curves smoothing, absence of resonances and changes in the SW properties. In particular, at large values of collision frequency the optical SW mode is degenerated due to the peculiarities of the semiconductor components of permittivity (ε_{f1} becomes positive in the neighborhood of hybrid frequency ω_g).

The imaginary part of the propagation constant k_x determines an attenuation constant (AC) of SW λ'. The maximum value of SW AC reaches 190 μm at $\nu = 5 \cdot 10^{10}\,\text{s}^{-1}$ and 100 μm at $\nu = 1 \cdot 10^{11}\,\text{s}^{-1}$. That is, with increasing electron collision frequency in the semiconductor layer, the AC of SW decreases. The AC becomes large at the transmission bands boundaries then decreases when approaching the characteristic frequencies $\omega_{s1,2}$ and becomes minimum at the boundaries of SW existence.

It should be noted that by means of external magnetic field one can effectively control the value of AC and PD into the multilayer periodic structure.

7. CONCLUSIONS

In summary, we have studied the properties of SW that are localized at the interface between the finite multilayered periodic structure and vacuum. It has been shown that there are two frequency ranges of SW which are characterized by several characteristic frequencies and magnetic fields and located below and above plasma frequency.

The effect of dissipation in the layers on the PD and AC of SW has been examined. It has been shown that by means of frequency, magnetic field, and thicknesses of the layers one can effectively control the parameters of SW as well as physical parameters of the considered structure. In addition, the distribution of SW field and the complex Poynting energy flux in the layered periodic structure were discussed. It was found that the complex energy flux can be concentrated on the right- or left-edge boundary of the structure depending on frequency, magnetic field and physical parameters of the structure.

The presence of resonance phenomena of different origin in the studied structure allows their use for numerous practical and technology application, for example, as electronically controllable microwave and optical devices, waveguides, frequency filters, etc..

REFERENCES

1. Armstrong, C. M., "The truth about terahertz," *IEEE Spectrum*, Vol. 49, No. 9, 28–33, 2012.
2. Konopsky, V. N., T. Karakouz, E. V. Alieva, C. Vicario, S. K. Sekatskii, and G. Dietler, "Photonic crystal biosensor based on optical surface waves," *Sensors*, Vol. 13, 2566–2578, 2013.
3. Chen, Y.-H., J.-X. Fu, and Z.-Y. Li, "Surface wave holography on designing subwavelength metallic structures," *Optics Express*, Vol. 19, No. 24, 23908–23920, 2011.
4. Su, S., L. Tang, and T. Yoshie, "Optical surface bloch modes of complete photonic bandgap materials as a basis of optical sensing," *Opt. Lett.*, Vol. 36, 2266–2268, 2011.
5. Hajian, H., B. Rezaei, A. S. Vala, and M. Kalafi, "Tuned switching of surface waves by a liquid crystal cap layer in one-dimensional

photonic crystals," *Applied Optics*, Vol. 51, No. 15, 2909–2916, 2012.

6. Usievich, B. A., V. V. Svetikov, D. K. Nurligareev, and V. A. Sychugov, "Surface waves on the boundary of photonic crystals and tunnelling coupling between two photonic crystals via these waves," *Quantum Electronics*, Vol. 39, No. 1, 94–97, 2009.
7. Zhang, X.-C., "Terahertz wave imaging: Horizons and hurdles," *Phys. Med. Biol.*, Vol. 47, 3667–3677, 2002.
8. Engheta, N. and R. Ziolkowski, *Metamaterials: Physics and Engineering Explorations*, Wiley, IEEE Press, Piscataway, NJ, 2006.
9. Bass, F. G. and A. A. Bulgakov, *Kinetic and Electrodynamic Phenomena in Classical and Quantum Semiconductor Superlattices*, Nova Science, New York, 1997.
10. Grzegorczyk, T. M. and J. A. Kong, "Review of left-handed metamaterials: Evolution from theoretical and numerical studies to potential applications," *Journal of Electromagnetic Waves and Applications*, Vol. 20, No. 14, 2053–2064, 2006.
11. Reinhard, B., O. Paul, R. Beigang, and M. Rahm, "Experimental and numerical studies of terahertz surface waves on a thin metamaterial film," *Optics Letters*, Vol. 35, 1320–1322, 2010.
12. Zhu, W., A. Agrawal, and A. Nahata, "Planar plasmonic terahertz guided-wave devices," *Opt. Express*, Vol. 16, No. 9, 6216–6226, 2008.
13. Ziolkowski, R. W. and E. Heyman, "Wave propagation in media having negative permittivity and permeability," *Phys. Rev. E*, Vol. 64, No. 5, 056625(15), 2001.
14. Bulgakov, A. A., A. A. Girich, M. K. Khodzitsky, O. V. Shramkova, and S. I. Tarapov, "Transmission of electromagnetic waves in a magnetic fine-stratified structure," *J. Opt. Soc. Am. B*, Vol. 26, No. 12, B156–B160, 2009.
15. Shramkova, O. V., "Transmission spectra in ferrite-semiconductor periodic structure," *Progress In Electromagnetics Research M*, Vol. 7, 71–85, 2009.
16. Pendry, J. B., "Negative refraction makes a perfect lens," *Phys. Rev. Lett.*, Vol. 85, 3966–3969, 2000.
17. Markos, P. and C. M. Soukoulis, *Wave Propagation: From Electrons to Photonic Crystals and Left-handed Materials*, Princeton University Press, New Jersey, 2008.
18. Ishimaru, A., J. R. Thomas, and S. Jaruwatanadilok, "Electromagnetic waves over half-space metamaterials of arbitrary per-

mittivity and permeability," *IEEE Transactions on Antennas and Propagations*, Vol. 53, No. 3, 915–921, Mar. 2005.

19. Darmanyan, S. A., M. Neviere, and A. A. Zakhidov, "Surface modes at the interface of conventional and left-handed media," *Optics Communications*, Vol. 225, 233–240, 2003.
20. Agranovich, V. M. and D. L. Mills, *Surface Polaritons. Electromagnetic Waves at Surfaces and Interfaces*, North-Holland, Amsterdam, 1982.
21. Pacheco, J., T. M. Grzegorzcyk, B. I. Wu, Y. Zhang, and J. A. Kong, "Wave propagation in homogeneous isotropic frequency-dispersive left-handed media," *Phys. Rev. Lett.*, Vol. 89, No. 25, 257401(4), 2002.
22. Iorsh, I. V., P. A. Belov, A. A. Zharov, I. V. Shadrivov, and Y. S. Kivshar, "Nonlinear Tamm states in nanostructured plasmonic metamaterials," *Phys. Rev. A*, Vol. 86, No. 2, 023819(6), 2012.
23. Zhou, L. and C. T. Chan, "High-impedance reflectivity and surface-wave band gaps in metamaterials," *Applied Physics Letters*, Vol. 84, No. 9, 1444–1446, Mar. 1, 2004.
24. Sievenpiper, D., L. Zhang, R. F. J. Broas, N. G. Alexopolous, and E. Yablonovitch, "High-impedance electromagnetic surfaces with a forbidden frequency band," *IEEE Transactions on Microwave Theory & Techniques*, Vol. 47, No. 11, 2059–2074, 1999.
25. Pendry, J. B., L. Martın-Moreno, and F. J. Garcia-Vidal, "Mimicking surface plasmons with structured surfaces," *Science*, Vol. 305, 847–848, 2004.
26. Navarro-Cia, M., M. Beruete, S. Agrafiotis, F. Falcone, M. Sorolla, and S. A. Maier, "Broadband spoof plasmons and subwavelength electromagnetic energy confinement on ultrathin metafilms," *Opt. Express*, Vol. 17, No. 20, 18184–18195, 2009.
27. Ishimaru, A., S. Jaruwatanadilok, and Y. Kuga, "Generalized surface plasmon resonance sensors using metameterials and negative index materials," *Progress In Electromagnetics Research*, Vol. 51, 139–152, 2005.
28. Hudlicka, M., J. Machac, and I. S. Nefedov, "A triple wire medium as an isotropic negative permittivity metamaterial," *Progress In Electromagnetics Research*, Vol. 65, 233–246, 2006.
29. Baccarelli, P., P. Burghignoli, F. Frezza, A. Galli, P. Lampariello, G. Lovat, and S. Paulotto, "Fundamental modal properties of surface waves on metamaterial grounded slabs," *IEEE Trans. Microwave Theory Tech.*, Vol. 53, No. 4, 1431–1442, 2005.

30. Woldeyohannes, M., J. Schenk, R. Ingel, S. Rigdon, M. Pate, J. Graham, M. Clare, W. Yang, and M. Fiddy, "Internal field distribution measurement in 1-D strongly anisotropic subwavelength periodic structures of finite length," *Optics Express*, Vol. 19, No. 1, 81–92, 2011.
31. Francisco, V. and J. A. Gaspar-Armenta, "Electromagnetic surface waves: Photonic crystal-photonic crystal interface," *Optics Communications*, Vol. 223, 109–115, 2003.
32. Gaspar-Armentaa, J. A., F. Villaa, and T. Lopez-Ros, "Surface waves in finite one-dimensional photonic crystals: Mode coupling," *Optics Communications*, Vol. 216, 379–384, 2003.
33. Meessen, A., "Production of EM surface waves by superconducting spheres: A new type of harmonic oscillators," *Progress In Electromagnetics Research Symposium Proceedings*, 529–533, Moscow, Russia, Aug. 19–23, 2012.
34. Averkov, Yu. O., V. M. Yakovenko, V. A. Yampol'skii, and F. Nori, "Oblique surface Josephson plasma waves in layered superconductors," *Phys. Rev. B*, Vol. 87, 054505(8), 2013.
35. Mousa, H. M., "Stability of nonlinear TE surface waves along the boundary of left-handed material," *Optics and Photonics Journal*, Vol. 2, No. 2, 123–128, 2012.
36. Liu, X. X., C. F. Tsai, R. L. Chern, and D. P. Tsai, "Dispersion mechanism of surface magnetoplasmons in periodic layered structures," *Applied Optics*, Vol. 48, No. 16, 3102–3107, 2009.
37. Bulgakov, A. A. and O. V. Shramkova, "Reflection coefficient of a semiconductor superlattice subjected to a magnetic field," *Semiconductors*, Vol. 34, No. 6, 686–692, 2000.
38. Yariv, A., P. Yeh, and C.-S. Hong, "Electromagnetic propagation in periodic stratified media," *J. Opt. Soc. Am.*, Vol. 67, No. 4, 423, 1977.
39. Stratton, J. A., *Electromagnetic Theory*, McGraw-Hill Book Company, Inc., New York and London, 1953.
40. Collin, R. E., *Field Theory of Guided Waves*, IEEE Press, New York, 1991.
41. Fedorin, I. V. and A. A. Bulgakov, "Surface plasmon polaritons in subwavelength semiconductor-dielectric periodic structure in an external magnetic field," *Proc. of Metamaterials 2012 Congress*, 288–290, St. Petersburg, Russia, 2012.